The effects of neutral gas heating on H mode transition and maintenance currents in a 13.56MHz planar coil inductively coupled plasma reactor

Kanesh K. Jayapalan and Oi-Hoong Chin

Citation: Phys. Plasmas **19**, 093501 (2012); doi: 10.1063/1.4750055
View online: http://dx.doi.org/10.1063/1.4750055
View Table of Contents: http://pop.aip.org/resource/1/PHPAEN/v19/i9
Published by the American Institute of Physics.

The effects of neutral gas heating on H mode transition and maintenance currents in a 13.56 MHz planar coil inductively coupled plasma reactor

Kanesh K. Jayapalan[a] and Oi-Hoong Chin[b]
Plasma Technology Research Centre, Department of Physics, University of Malaya, 50603 Kuala Lumpur, Malaysia

(Received 22 May 2012; accepted 20 August 2012; published online 12 September 2012)

The H mode transition and maintenance currents in a 13.56 MHz laboratory 6 turn planar coil inductively coupled plasma (ICP) reactor are simulated for low pressure argon discharge range of 0.02–0.3 mbar with neutral gas heating and at ambient temperature. An experimentally fitted 3D power evolution plot for 0.02 mbar argon pressure is also shown to visualize the effects of hysteresis in the system. Comparisons between simulation and experimental measurements show good agreement in the pressure range of 0.02–0.3 mbar for transition currents and 0.02–0.1 mbar for maintenance currents only when neutral gas heating is considered. This suggests that neutral gas heating plays a non-negligible role in determining the mode transition points of a rf ICP system. © *2012 American Institute of Physics*. [http://dx.doi.org/10.1063/1.4750055]

I. INTRODUCTION

Radio frequency or rf inductively coupled plasmas (ICPs) have been extensively used since the past two decades for various semiconductor processes including plasma enhanced chemical vapor deposition (PECVD) and reactive ion etching (RIE). These processes demand high purity and high density plasmas which are able to give the precise (up to nanometer scale) substrate modification required for fabricating present day electronic devices. Inductively coupled plasmas being electrode-less (i.e., without direct contact with source electrode, thus, having reduced impurities) are induced mainly by the magnetic field of an external coil and are effectively able to generate high density ranged plasmas of 10^{17}–$10^{19}\,m^{-3}$ (Refs. 1–4).

ICPs in practice (despite being primarily inductive) have both capacitive and inductive means of power coupling which together contribute towards the overall plasma. The primary mode of the plasma (known as the H mode) is generated via predominant inductive coupling of the magnetic fields of the rf coil. The secondary of the plasma (known as the E mode) is generated via a radial electric (electrostatic or capacitive) field formed by the potential difference across the coil. The E mode is usually found at lower input powers where ionization from the potential difference of the coil is insufficient to ignite the inductive discharge and power coupling from the electromagnetic fields of the coil is low.[1] An ICP at H mode and at E mode can be differentiated by distinct features in electron density and luminosity. At H mode, the plasma is highly luminous and has a high electron density (10^{17}–$10^{19}\,m^{-3}$), whereas at E mode, the plasma is at low luminosity and has an electron density of about one to two orders lower. Transitions between E mode and H mode occur in sudden "jumps" of luminosity when a threshold input power (input coil current) is applied. The threshold current which triggers these jumps depends not only on external parameters (i.e., gas pressure, coil size, impedance matching, and gas type) but also on whether the input current is incremented or decremented. This hysteresis phenomenon has become a point of interest for many researchers in this field of study and is well documented.[5–10]

With the advent of newer spectroscopic measurement techniques, neutral gas temperatures in ICPs have been measured to be significantly higher than room temperature, with temperatures reaching up to 1850 K in some cases.[11] Neutral gas heating in ICPs (which strongly correlates to neutral gas depletion, especially at pressures above 0.01 mbar) has also been found to impact not only the intrinsic properties of the plasma such as electron density and electron temperature distributions[12,13] but also the transitions between modes.[14] However, the effects of neutral gas heating and/or neutral gas depletion on mode transitions have yet to be simulated.

In this study, we simulate the H mode transition (E to H mode jump) and maintenance (H to E mode jump) currents of an argon discharge within a laboratory planar coil ICP reactor (Fig. 1) at the low pressure range of 0.02–0.3 mbar. Calculations have been made to take into account the power contributions of H mode, E mode, and stochastic heating of plasma electrons via capacitive sheath, the nonlinear effects of electron energy distribution towards power balance and the effects of neutral gas heating. The simulated results are compared and matched with experimental measurements. Hysteresis in the system is also demonstrated via a modeled 3D power evolution plot at 0.02 mbar argon pressure.

II. ICP SETUP

The coil used in experiment is a 6 turn planar coil which is driven by a 600 W, 13.56 MHz rf generator (Model AG0613). The system has a manual matching circuit with a variable air capacitor to adjust impedance. A rf compensated Langmuir probe (0.5 mm diameter tungsten wire with

[a]E-mail: kane_karnage@yahoo.com.
[b]E-mail: ohchin@um.edu.my.

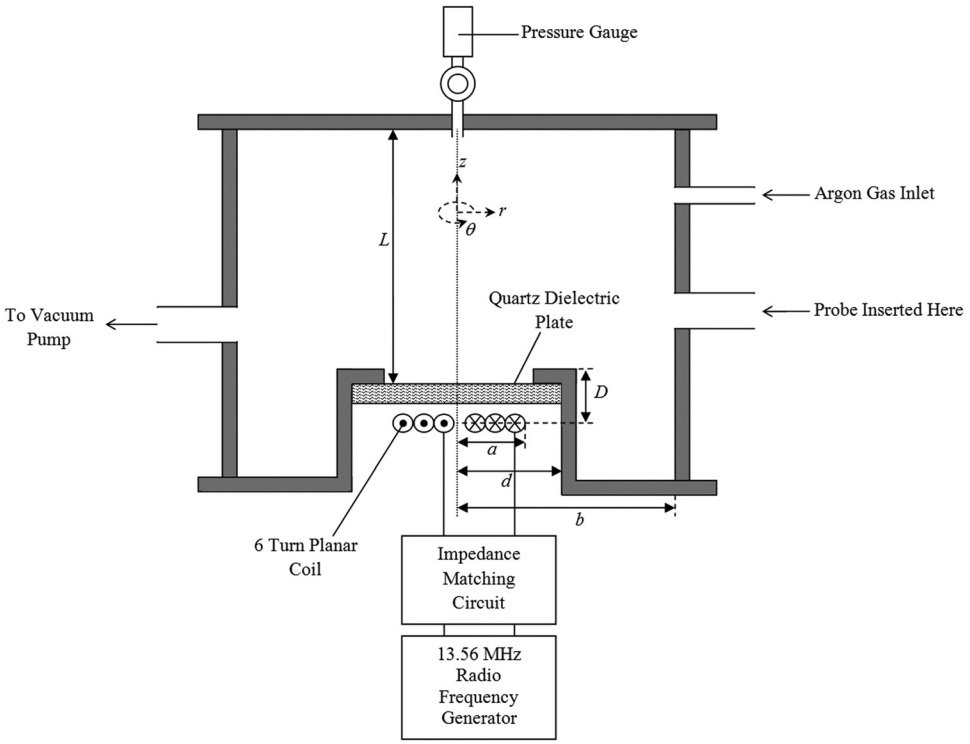

FIG. 1. Schematic diagram of the laboratory 13.56 MHz, 6 turn planar coil, inductively coupled plasma reactor. The simulated chamber is azimuthally symmetric (r and z only) with a planar coil radius, $a = 4.5$ cm, dielectric radius, $d = 10.0$ cm, chamber radius, $b = 14.5$ cm, effective chamber height, $L = 21.8$ cm and coil-chamber distance, $D = 2.4$ cm.

a collecting area of 4.76 mm^2) was used to measure the electrical characteristics of the plasma to obtain the electron temperature for simulation.[15] Neutral gas temperatures were measured by actinometry technique.[11,16,17] The optical emission spectra were viewed through a quartz diagnostic port at the same level as the Langmuir probe. The spectra were recorded by the Ocean Optics HR4000 spectrometer with 600 lines/mm^{-1} grating and 10 μm slit width via an optical fiber cable mounted with a collimator. Measurement of H mode transition and maintenance currents was made using a current transformer (Model Pearson 6595).

III. THEORETICAL MODEL

In an ICP system, the stable operating conditions (as seen in experiments) are theorized to be the points at which equilibrium is achieved between the total absorbed electron power and electron power loss; with both being non-linear functions of electron density. Total absorbed electron power is derived primarily from components that contribute to the heating of the electrons. For ICP simulations, the combination of H mode power, E mode power, and stochastic heating of the plasma's capacitive sheath is typically considered and is described by Eqs. (1)–(6) of which the details including the derivation of the effective electron collision frequency can be found in the Appendix.[18–20] To calculate the average H mode and E mode absorbed electron powers, the Poynting vector ($1/\mu_0 \boldsymbol{E} \times \boldsymbol{B}$ or resultant energy flux density in Wm^{-2} into the plasma) is integrated over the coil area. The respective H mode and E mode power, P_h and P_e, coupled into the plasma can be summarized as[19]

$$P_h = \mathrm{Re}\left(-\pi K_\theta \int_0^a r E_\theta(r, L+D)\delta r \right), \tag{1}$$

and

$$P_e = \mathrm{Re}\left(-\frac{2\pi}{\mu_o} E_o \int_0^a r B_\theta^*(r, L+D)\delta r \right), \tag{2}$$

where K_θ is the equivalent surface current generated by the coil and is given by $K_\theta = NI_p/a$, N being the number of turns in the coil, I_p the peak coil current in A, and a the coil radius in m. μ_0 is the vacuum permeability in TmA^{-1} and B_θ* is the conjugate azimuthal magnetic field in T. E_o is the electric field across the coil radius in Vm^{-1}; given by $E_o = V/a$ where, V is the voltage across the rf coil in V and a is the coil radius in m. At lower electron densities, the plasma sheath (generated by the capacitive voltage of the coil) plays a significant role in damping the emitted H mode power from being absorbed by the plasma electrons. When computing the H mode power, a simplified time-averaged capacitive sheath thickness, S is added to the coil-chamber distance, D to model this effect. It is expressed as

$$S = \frac{1}{a}\int_0^a \frac{5J_s^3(r)}{12e^2\omega^3\varepsilon_o\ n_e^2 T_e}\delta r, \tag{3}$$

where ε_o is the vacuum permittivity in C^{2}N^{-1}m^{-2}, ω is the rf angular frequency (rads^{-1}), and T_e is the electron temperature of the plasma in eV. J_s is first harmonic component of current density through the sheath and is given by,

$$J_s^2(r) \approx 1.73 e\varepsilon_o\omega^2 n_e \left(\frac{T_e V_s(r)}{a}\right)^{1/2}, \tag{4}$$

where $V_s(r)$ is the first harmonic component of voltage across the plasma sheath at the coil-dielectric interface.[1,19] In addition

to the power absorbed from H mode and E mode, electrons are also heated by acceleration when inside the oscillating capacitive sheath of the plasma. The resultant power gain from this stochastic heating of the plasma sheath is given by,

$$P_{\text{stoc}} \approx 0.9\pi a^2 \varepsilon_o \omega^2 \left(\frac{m_e T_e}{e}\right)^{1/2} \int_0^a V_s(r)\pi r \delta r. \quad (5)$$

By summing the component powers of Eqs. (1), (2), and (5), the total power absorbed by the electrons can be written as

$$P_{\text{abs}} = P_h + P_e + P_{\text{stoc}}. \quad (6)$$

Electron power loss in an ICP is primarily due to the energy dissipated for the sustenance and creation of ion-electron pairs in the discharge. In simplified derivations, this power dissipation, P_{loss} is directly proportional to the electron density, n_e (i.e., $P_{\text{loss}} \propto n_e$). However, in order to successfully simulate hysteresis in a plasma system, non-linearities in the power loss curve have to be taken into consideration. For this simulation, the contribution of electron-electron collisions or Coulomb collisions is considered; with the transition from Druyvestyen to Maxwellian electron energy density function (EEDF) being representative of the non-linearity in the electron power loss.[5,7,21] This equation for P_{loss} can be written as,

$$P_{\text{loss}} = n_e u_B A_{\text{eff}} \varepsilon_{T_e} \left(\frac{\varepsilon_{cD}}{\varepsilon_{cM}}\right)^{1/(1+x n_e/n_g)}, \quad (7)$$

where u_B is the Bohm velocity in ms^{-1} given by $u_B = (eT_e/M_{Ar})^{1/2}$ with M_{Ar} being the argon ion mass in kg. A_{eff} is the effective surface area of the plasma in m^2 and ε_{Te} is the total collisional electron energy lost per electron-ion pair created by the discharge in J and is dependent on electron temperature, T_e.[7] The non-linear term, $(\varepsilon_{cD}/\varepsilon_{cM})^{1/(1+x n_e/n_g)}$, accounts for the transition of the EEDF from Druyvesteyn to Maxwellian at increasing electron density with the factor x being heuristically chosen to be in the 10^4–10^5 range so that the transition occurs near $n_e \approx 10^{15}$–10^{16} for our range of pressures.[21] x represents the experimental discrepancy of the transition point between EEDFs which is simplified in this simulation. Here, ε_{cD} and ε_{cM} are the Druyvesteyn and Maxwellian electron-electron collision energy loss factors and n_g is the neutral argon gas density in m^{-3}. n_g is determined from argon filling pressure, P and neutral gas temperature, T_n i.e., $n_g \approx P/k_B T_n$ where k_B is the Boltzmann constant.[12,16]

When the absorbed electron energy and electron energy loss parameters are plotted against electron density, they intersect at certain points in which both energies are at equilibrium ($P_{\text{abs}} = P_{\text{loss}}$). These intersecting points represent the plausible operating states (being E mode or predominantly coupled by P_e at lower electron densities and H mode or predominantly coupled by P_h at higher electron densities) of the system observable in experiments. Plausibility of these operating points also depends on the condition of stability in which the rate of change of absorbed power with electron density must be less than the rate of change of power loss with electron density (i.e., $\delta P_{\text{abs}}/\delta n_e < \delta P_{\text{loss}}/\delta n_e$).[7,22] An illustrative of this is seen in Fig. 2, where points I and III

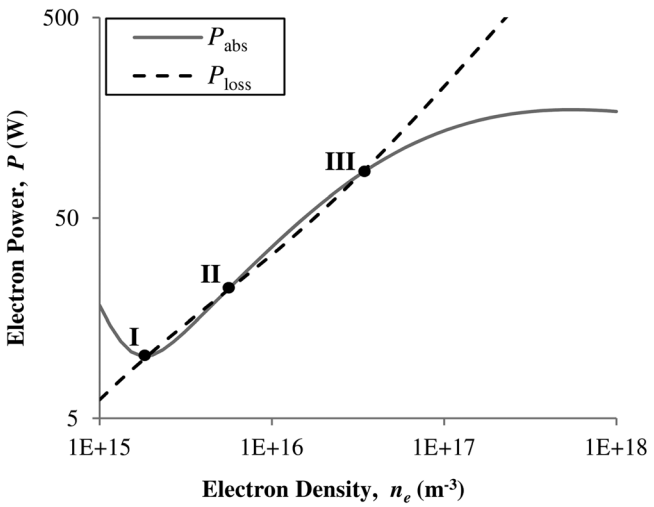

FIG. 2. Simulated electron absorbed power and electron power loss versus electron density for 15 A peak rf coil current at 0.02 mbar argon pressure. I, II, and III represent the E mode, unstable operation, and H mode, respectively. Electron temperature, T_e, neutral gas temperature, T_n, and the factor x (as in Eq. (7)) were set at 4.2 eV, 433 K, and 6.6×10^4, respectively.

represent the stable and observable H and E mode operations, respectively, with $\delta P_{\text{abs}}/\delta n_e < \delta P_{\text{loss}}/\delta n_e$ and $P_{\text{abs}} = P_{\text{loss}}$ conditions fulfilled. Point II represents an unstable state which is not observable experimentally.

IV. ELECTRON TEMPERATURE MEASUREMENTS FOR SIMULATION

The electron temperature values used in simulation were estimated within the range of measured experimental values. A laboratory Langmuir probe mounted at 3.2 cm axial height from the dielectric plate was used to obtain radial measurements at 1 cm intervals for 0.03 mbar, 0.07 mbar, and 0.2 mbar argon pressures with rf power set at 180 W (Fig. 3).

V. DETERMINATION OF NEUTRAL GAS TEMPERATURE USING OPTICAL EMISSION SPECTROSCOPY (OES)

Simulation of the effects of neutral gas heating on H mode transition and maintenance currents was done using

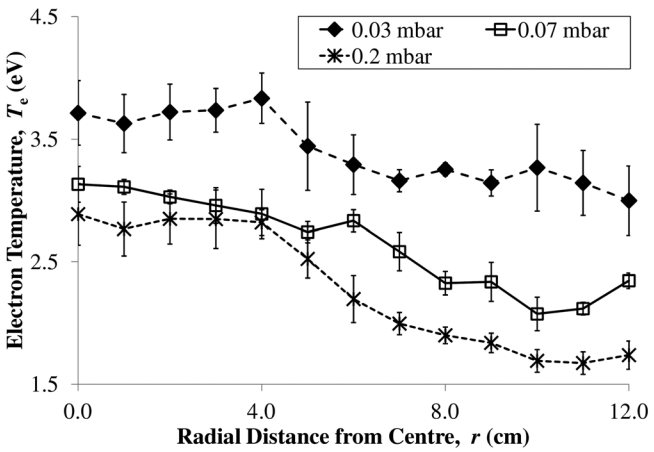

FIG. 3. Measured radial electron temperature, T_e for 0.03, 0.07, and 0.2 mbar argon pressure at 180 W rf power (at H mode).

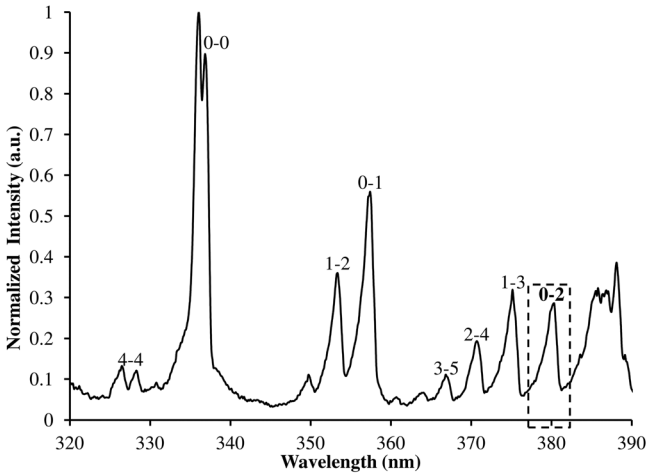

FIG. 4. Measured emission spectra for the nitrogen second positive system ($N_2C^3\Pi_u$-$N_2B^3\Pi_g$) at 0.05 mbar filling pressure and 200 W rf power (H mode).

the neutral gas temperatures within the range indicated by experimentally measured data. Experimental data were obtained by using the actinometry technique demonstrated by previous workers.[11,16,17] About 4%–5% nitrogen gas was seeded with argon at 0.03, 0.05, and 0.1 mbar filling pressure and the resultant plasma emission was recorded using the OES system. The second positive band emission of nitrogen located near 380 nm ($N_2C^3\Pi_u$-$N_2B^3\Pi_g$ at $v' = 0$ and $v'' = 2$) was used for neutral gas temperature determination due to the relatively impurity free characteristics of the spectra (Fig. 4).[23] Measured neutral gas temperatures for increasing and decreasing rf powers are shown in Figs. 5 and 6. Error was in the range of 10%–20% for E mode and 5%–12% for H mode.

VI. HYSTERESIS AND THE DETERMINATION OF H MODE TRANSITION AND MAINTENANCE CURRENTS

In order to determine the H mode transition current (i.e., minimum current required to jump from E to H mode) and H mode maintenance current (i.e., minimum H mode current

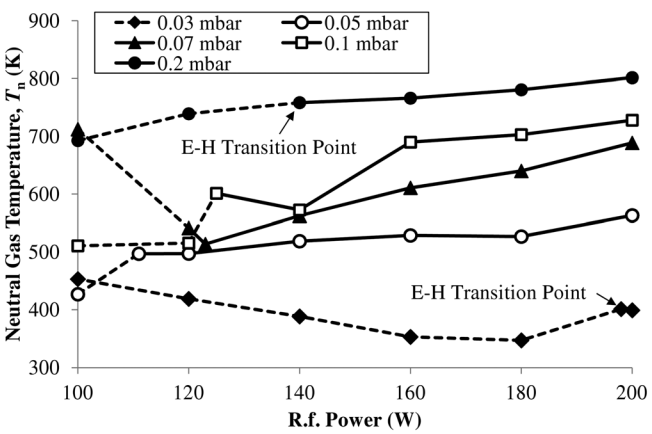

FIG. 5. Measured neutral gas temperatures at 0.03, 0.05, 0.07, 0.1, and 0.2 mbar filling pressure for the increasing rf power range of 100–200 W. The solid and dashed lines denote H and E modes, respectively. The data point separating the solid and dashed lines is measured at H mode, immediately after E-to-H mode transition.

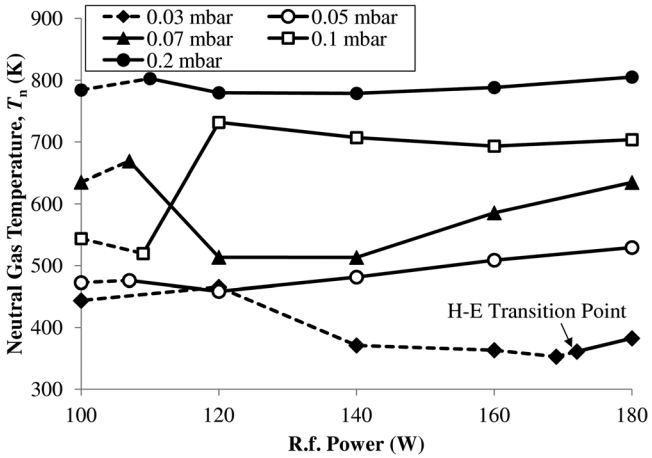

FIG. 6. Measured neutral gas temperatures at 0.03, 0.05, 0.07, 0.1, and 0.2 mbar filling pressure for the decreasing rf power range of 200-100 W. The solid and dashed lines denote H and E modes, respectively. The data point separating the solid and dashed lines is measured at E mode, immediately after H-to-E mode transition.

before transition to E mode), it is important to have an understanding on the mechanism of hysteresis in the ICP system. Taking the experimentally fitted case of 0.02 mbar argon pressure as an example, a 3D plot of electron power (absorbed and loss) versus peak coil current and electron density is first visualized (Fig. 7).

The magenta (lighter) surface of the 3D plot represents the absorbed electron power evolution, whereas dark blue (darker) surface represents the electron power loss evolution. As aforementioned, the intersections between the two surfaces represent the working path of the system. In a typical experiment, the input coil current starts at zero. As the input coil current (or rf power) is increased, the operating point of the system moves to point 1 (Figs. 7 and 8). At this point, the low density E mode plasma is observed (E mode was ignited before point 1 at input coil current of 5.2 ± 0.2 A). A further increase in current would shift the operating point of the system to point 2. Point 2 is the threshold at which any further increase in coil current would trigger a transition from E to H mode, marking the H mode transition current (Figs. 7 and 9).

From point 2, the system jumps to point 3 which is in H mode. Point 3 is determined experimentally and is affected by the sensitivity and accuracy of the impedance matching circuit.[7,19,21] Increase in coil current at point 3 would bring system operation to point 4 (Figs. 7 and 8) which is higher density plasma in H mode. When coil current is decreased from point 4, the system follows the working H mode path until point 5. Point 5 is the threshold at which a further decrease would trigger a transition to E mode (Figs. 7 and 9). This threshold point is measured as the minimum or maintenance current for H mode plasma. The difference between transition and maintenance currents seen in the plot denotes the effects of hysteresis in the system. From point 5, a decrease in coil current shifts the system operation to point 6 which is in E mode.

It is noted that the experimentally measured H mode transition and maintenance currents for 0.02 mbar argon pressure are 16.4 ± 0.1 A and 14.3 ± 0.3 A, respectively,

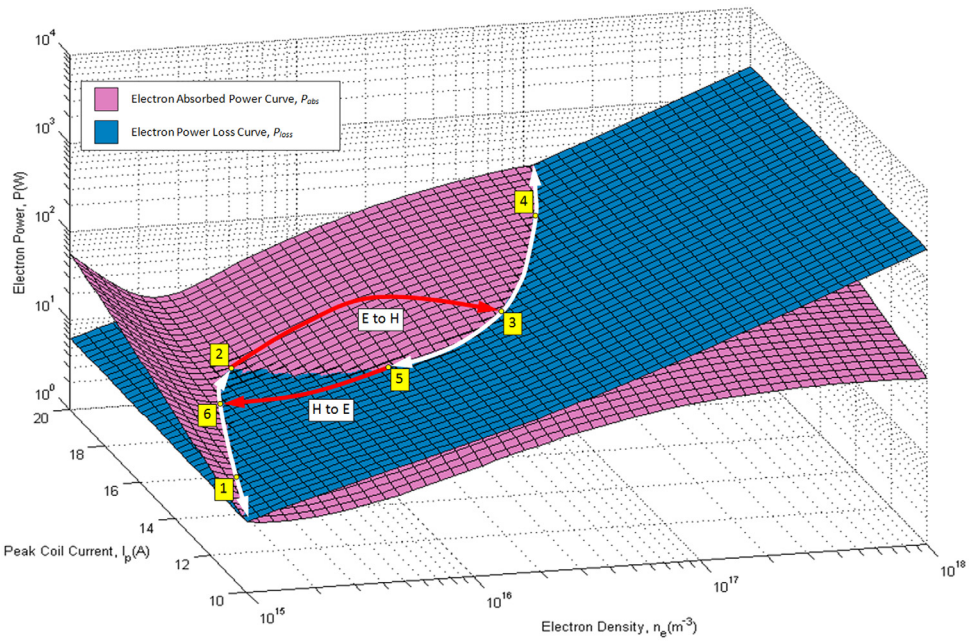

FIG. 7. A 3D plot of absorbed electron power, P_{abs} (magenta surface) and electron power loss, P_{loss} (dark blue surface) versus electron density, n_e and peak coil current, I_p at 0.02 mbar argon pressure. Electron temperature, T_e was set at 4.2 eV, neutral gas temperature, T_n set at 433 K and $x = 6.6 \times 10^4$. The white arrows indicate the working path of the system, whereas the red arrows indicate mode transitions.

and these are consistent with the simulated values (16.41 A and 14.19 A) presented in this example.

VII. H MODE TRANSITION AND MAINTENANCE CURRENTS VERSUS PRESSURE

For the main analysis in this paper, the H mode transition and maintenance currents are measured for the argon pressure range of 0.02–0.3 mbar and compared with simulation (Figs. 10 and 11). The plasma parameters used in simulation of the H mode transition current curve are $T_e = 4.0$ eV, $T_n = 583$ K, and $x = 8.8 \times 10^4$, whereas for the H mode maintenance current curve, the parameters are $T_e = 3.0$ eV, $T_n = 623$ K, and $x = 3.0 \times 10^5$. Values for electron temperature and neutral gas temperature for both cases were taken within experimentally measured range, whereas the values for x were chosen heuristically within the previously mentioned order. For further comparison, simulation at ambient temperatures ($T_n = 298$ K) for both H mode transition and maintenance current curves is also shown.

From Figs. 10 and 11, it is observed that the simulated H mode transition (for the argon pressure range of 0.02–0.3 mbar) and maintenance (for the argon pressure range of 0.02–0.1 mbar) curves are well matched to experimental values when neutral gas heating is considered. Transition and maintenance curves at ambient temperature, however, are not well matched. At lower filling pressures for the H mode transition curve (<0.06 mbar), it is seen that the experimentally measured currents are higher than the currents simulated at ambient temperature. In experiment, thermalization of the neutrals diffuses the particles in the plasma in accordance to ideal gas law. Since, the plasma is diffuse, higher input current is required to generate sufficient plasma ionization (i.e., reach threshold electron density) to attain H

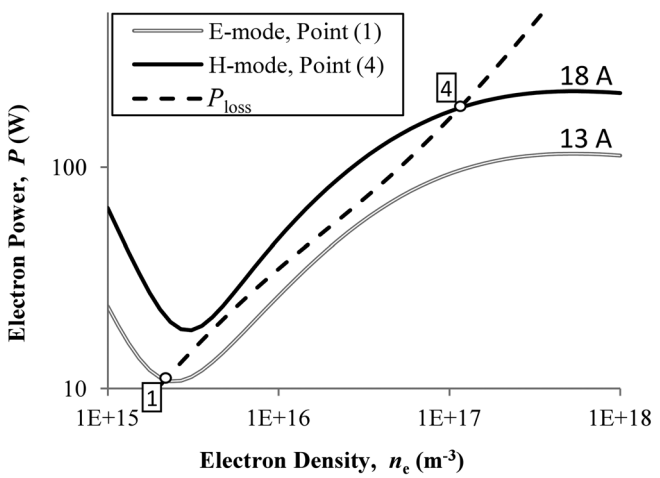

FIG. 8. The simulated absorbed electron power (full line) and power loss (dashed line) curves depicting the current at which either E-mode (point 1 at 13 A) or H-mode (point 4 at 18 A) operation alone occurs.

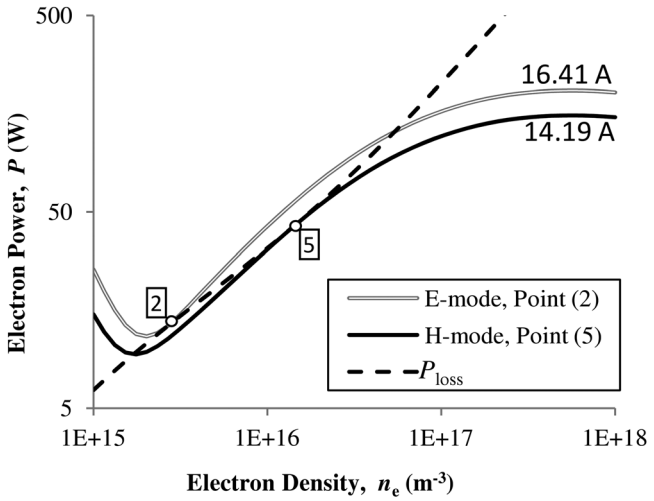

FIG. 9. The simulated absorbed electron power (full line) and power loss (dashed line) curves depicting the threshold currents for E to H (point 2 at 16.41 A; H mode transition current) and H to E (point 5 at 14.19 A; H mode maintenance current) mode transitions.

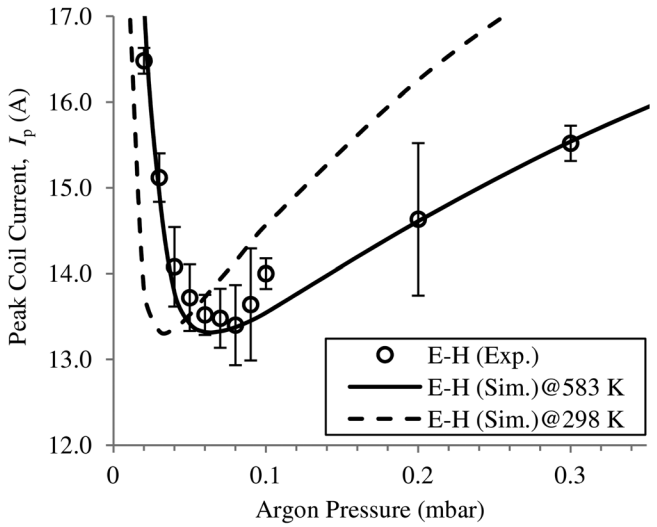

FIG. 10. Simulated (Sim.) and experimentally (Exp.) measured H mode transition (E-H) curves for the argon pressure range of 0.02–0.3 mbar. Neutral gas temperatures for the simulated curves were set at 583 K and 298 K.

mode.[24] At higher filling pressures for the H mode transition curve (>0.06 mbar), the neutral gas density of the plasma has become high enough such that thermalization of the neutral particles increases the power transfer efficiency by assisting plasma collisional processes.[1,25] This reduces the input currents required to sustain H mode.

Mismatch between measured H mode maintenance currents and simulated H mode maintenance currents at ambient temperature can also be explained in the same way as the H mode transition curve, with thermalization of the neutrals in experiment diffusing the plasma (i.e., higher measured input current) at lower filling pressures (<0.09 mbar) and assisting in plasma collision processes (i.e., lower measured input current) at higher filling pressures (>0.09 mbar). The higher pressure region at which diffusion of the particles influence the H mode maintenance currents (~0.09 mbar) as compared

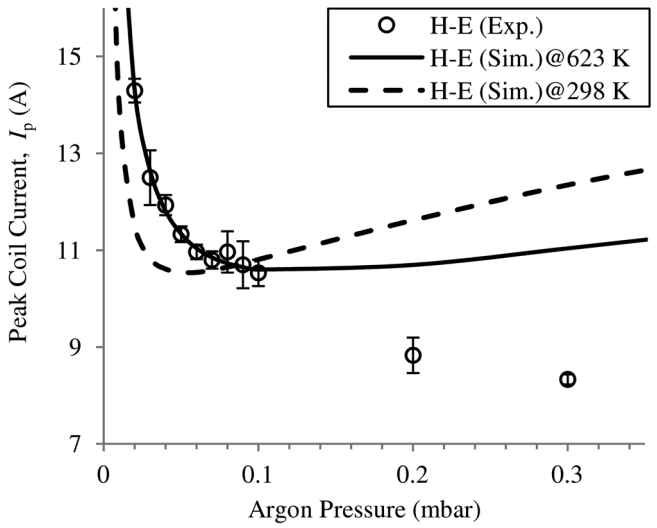

FIG. 11. Simulated (Sim.) and experimentally (Exp.) measured H mode maintenance (H-E) curves for the argon pressure range of 0.02–0.3 mbar. Neutral gas temperatures for the simulated curves were set at 623 K and 298 K.

to the H mode transition currents (~0.06 mbar) is due to the lower plasma density at which the H to E mode transition occurs.

The increasing deviation at higher pressures of 0.2–0.3 mbar between the fitted and experimental H mode maintenance curves is suspected to be due to the non-linear effects of multistep ionization which was not included in the simulation. At higher pressures, complex ionization processes occurring from intermediary or metastable excitation states become more significant such that the total energy required to sustain the ion-electron pairs created in the discharge is further reduced (i.e., lower electron power loss).[21] This effect, in part, explains the ability of the H mode discharge in experiment to be maintained at a much lower current than the values obtained by simulation.

VIII. CONCLUSION

In this paper, hysteresis occurring in the ICP plasma system was visualized via an experimentally matched, 3D power evolution surface plotted at 0.02 mbar argon pressure. Also, the simulation of H mode transition and maintenance currents in a 13.56 MHz laboratory 6 turn planar coil ICP reactor was done at the low pressure argon discharge range of 0.02–0.3 mbar for elevated (neutral gas heating) and ambient neutral gas temperature. Experimental results were in good agreement for the range of 0.02–0.3 mbar for transition currents and 0.02–0.1 mbar for maintenance currents for the simulation that included neutral gas heating. The mismatch of the maintenance currents at 0.2 and 0.3 mbar is suspected to be due to the non-linear effects of multistep ionization. When using ambient temperature, the simulations were poorly matched. It can be thus concluded that neutral gas heating plays a non-negligible role in determining the E to H and H to E mode transition points (i.e., H mode transition and maintenance currents) in an rf ICP system.

ACKNOWLEDGMENTS

This work is supported by the University of Malaya under the research Grant Nos. PS329-2010A and RG135-10AFR.

APPENDIX: ELECTROMAGNETIC FIELD DERIVATION

To calculate the H mode and E mode electromagnetic fields in the chamber (with reference to El-Fayoumi *et al.*),[18,19] the following assumptions were made:

1. The plasma is composed of immobile ions and cold electrons.
2. The electromagnetic field is simplified to follow local Ohm's Law.
3. The chamber is an azimuthally symmetrical cylinder.
4. Displacement current is ignored for the H mode fields due to the long free-space wavelength of the excitation frequency (~22 m for 13.56 MHz) in comparison to chamber dimensions. However, the displacement current flow through the dielectric quartz plate is considered when calculating the E mode fields.

The electromagnetic fields for both H mode and E mode can be thus expressed as

H mode:

$$\frac{1}{r}\frac{\partial}{\partial r}\left(r\frac{\partial E_\theta}{\partial r}\right)-\frac{E_\theta}{r^2}+\frac{\partial^2 E_\theta}{\partial z^2}=\alpha^2 E_\theta, \tag{A1}$$

$$B_r=-\frac{i}{\omega}\frac{\partial E_\theta}{\partial z}, \tag{A2}$$

$$B_z=\frac{i}{\omega}\frac{1}{r}\left(\frac{\partial(rE_\theta)}{\partial r}\right), \tag{A3}$$

for $0 \le z \le L+D$.

E mode:

$$\frac{1}{r}\frac{\partial}{\partial r}\left(r\frac{\partial B_\theta}{\partial r}\right)-\frac{B_\theta}{r^2}+\frac{\partial^2 B_\theta}{\partial z^2}=-\varepsilon_p\left(\frac{\omega}{c}\right)^2 B_\theta, \tag{A4}$$

$$E_r=\frac{ic^2}{\omega\varepsilon_p}\frac{\partial B_\theta}{\partial z}, \tag{A5}$$

$$E_z=-\frac{ic^2}{\omega\varepsilon_p}\frac{1}{r}\left(\frac{\partial(rB_\theta)}{\partial r}\right), \tag{A6}$$

for $0 \le z \le L$;

and

$$\frac{1}{r}\frac{\partial}{\partial r}\left(r\frac{\partial B_\theta}{\partial r}\right)-\frac{B_\theta}{r^2}+\frac{\partial^2 B_\theta}{\partial z^2}=-\varepsilon_r\left(\frac{\omega}{c}\right)^2 B_\theta, \tag{A7}$$

$$E_r=\frac{ic^2}{\omega\varepsilon_r}\frac{\partial B_\theta}{\partial z}, \tag{A8}$$

$$E_z=-\frac{ic^2}{\omega\varepsilon_r}\frac{1}{r}\left(\frac{\partial(rB_\theta)}{\partial r}\right), \tag{A9}$$

for $L < z \le L+D$.

Here, α^2 and ε_p are the spatial decay and plasma dielectric constants, respectively, and are given by,

$$\alpha^2=\frac{\mu_o n_e e^2}{m_e[1-i\nu/\omega]}, \tag{A10}$$

and

$$\varepsilon_p=1-\frac{c^2\mu_o n_e e^2}{m_e\omega^2[1-i\nu/\omega]}. \tag{A11}$$

ε_r is the dielectric constant of the quartz window which is taken as 3.8. μ_o is the vacuum permeability in NA^{-2}, n_e the electron density in m^{-3}, c is the speed of light in ms^{-1}, e the electronic charge in C, m_e the electronic mass in kg, and ν the effective electron collision frequency in Hz. The field equations were solved analytically by the separation of variables method using the following boundary conditions:

At the interface between the chamber walls and the plasma, the tangential electric field and normal magnetic fields are equal to zero.

1. The tangential electric fields and normal magnetic fields are continuous at the boundary between the quartz plate and plasma.
2. The coil is assumed to be an infinitely thin disc of radius, a with a surface current density of $K_\theta = NI_p/a$. The H mode radial magnetic field, B_r at $L+D$ can, thus, be simplified as, $B_r = -\mu_o K_\theta/2$.
3. A constant radial electrical field, E_r of amplitude, $E_r \equiv E_o = V/a$ is assumed across the coil at $L+D$.

1. Effective electron collision frequency, ν

The effective electron collision frequency, ν, is calculated by taking the sum of contributions of three components,[20] i.e., electron neutral collision frequency, ν_{en}, the electron ion collision frequency, ν_{ei}, and the stochastic collision frequency, ν_{st} and is expressed as

$$\nu=\nu_{en}+\nu_{ei}+\nu_{st}. \tag{A12}$$

The electron neutral collision frequency, ν_{en}, is dependent on the argon collision cross section and electron energy distribution and is given as,

$$\nu_{en}+i\omega=-\frac{3}{2\left[\int\frac{\varepsilon^{3/2}}{\nu_c(\varepsilon)+i\omega}\frac{df}{d\varepsilon}d\varepsilon\right]}, \tag{A13}$$

with ε being the electron energy in J and $f(\varepsilon)$ being the Maxwellian electron energy distribution. $f(\varepsilon)$ is expressed as,

$$f(\varepsilon)=\frac{2}{\sqrt{\pi}}\frac{1}{(eT_e)^{3/2}}e^{-\varepsilon/T_e}, \tag{A14}$$

where T_e is the electron temperature in eV. The term $\nu_c(\varepsilon)$ is the collision frequency of argon gas and is given by,

$$\nu_c(\varepsilon)=n_g\sigma_c(\varepsilon)\left(\frac{2e\varepsilon}{m_e}\right)^{1/2}. \tag{A15}$$

Here, n_g is the neutral gas density of the plasma in m^{-3} and σ_c is the collision cross section of argon gas in m^2 (Refs. 1 and 26). n_g is calculated from the ideal gas law, $n_g \approx P/k_B T_n$.[12,27] P is the argon filling pressure in Pa, k_B is the Boltzmann constant in JK^{-1}, and T_n is the neutral gas temperature in K.

[1] M. A. Lieberman and A. J. Lichtenberg (Wiley-Interscience, 2005) pp. 403–404, p. 462.
[2] J. Hopwood, Plasma Sources Sci. Technol. **1**, 109 (1992).
[3] J. Hopwood, Plasma Sources Sci. Technol. **3**, 460 (1994).
[4] J. Amorim, H. S. Maciel, and J. P. Sudano, J. Vac. Sci. Technol. B **9**, 362 (1991).
[5] U. Kortshagen, N. D. Gibson, and J. E. Lawler, J. Phys. D: Appl. Phys. **29**, 1224 (1996).
[6] A. M. Daltrini, S. A. Moshkalev, T. J. Morgan, R. B. Piejak, and W. G. Graham, Appl. Phys. Lett. **92**, 061504 (2008).
[7] G. Cunge, B. Crowley, D. Vender, and M. M. Turner, Plasma Sources Sci. Technol. **8**, 576 (1999).
[8] K. Ostrikov, E. Tsakadze, J. Ning, Z. Tsakadze, L. Jidong, R. Storer, and S. Xu, IEEE Trans. Plasma Sci. **30**, 128 (2002).
[9] H. C. Lee and C. W. Chung, Thin Solid Films (2012), doi:10.1016/j.tsf.2011.12.015.

[10]Y. W. Lee, H. L. Lee, and T. H. Chung, J. Appl. Phys. **109**, 113302 (2011).
[11]H. Li, C. Xiao, E. Zhang, A. K. Singh, and A. Hirose, Radiat. Eff. Defects Solids **166**, 399 (2011).
[12]D. O'Connell, T. Gans, D. L. Crintea, U. Czarnetzki, and N. Sadeghi, J. Phys. D: Appl. Phys. **41**, 035208 (2008).
[13]A. Fruchtman, G. Makrinich, P. Chabert, and J. M. Rax, Phys. Rev. Lett. **95**, 11500 (2005).
[14]K. A. MacKinnon, Philos. Mag. Ser. 7 **8**, 605 (1929).
[15]F. F. Chen, in IEEE-ICOPS Meeting, Jeju, Korea, 2003.
[16]M. Shimada, G. R. Tynan, and R. Cattolica, Plasma Sources Sci. Technol. **16**, 193 (2007).
[17]E. J. Tonnis and D. B. Graves, J. Vac. Sci. Technol. A **20**, 1787 (2002).
[18]I. M. El-Fayoumi and I. R. Jones, Plasma Sources Sci. Technol. **7**, 162 (1998).
[19]I. M. El-Fayoumi, I. R. Jones, and M. M. Turner, J. Phys. D: Appl. Phys. **31**, 3082 (1998).
[20]J. T. Gudmundsson and M. A. Lieberman, Plasma Sources Sci. Technol. **7**, 83 (1998).
[21]M. M. Turner and M. A. Lieberman, Plasma Sources Sci. Technol. **8**, 313 (1999).
[22]K. P. Shamrai, V. P. Pavlenko, and V. B. Taranov, Plasma Phys. Controlled Fusion **39**, 505 (1997).
[23]M. Shimada, Ph.D. dissertation, University of California, San Diego, 2006.
[24]A. Fruchtman, Plasma Sources Sci. Technol. **17**, 024016 (2008).
[25]K. Suzuki, K. Nakamura, H. Ohkubo, and H. Sugai, Plasma Sources Sci. Technol. **7**, 13 (1998).
[26]M. Hayashi, Inst. Plasma Phys., Nagoya University, Report IPPJ-AM-19 (Nov. 1981).
[27]M. Shimada, G. R. Tynan, and R. Cattolica, J. Appl. Phys. **103**, 033304 (2008).